PROCEEDINGS of the
23rd International Congress on Acoustics

9 to 13 September 2019 in Aachen, Germany

Numerical acoustic modelling of a ventilation unit by 3D FEM and application to the design of an ANC feedforward system

Stéphane LESOINNE[1]; Jean-Jacques EMBRECHTS[1]; Guillaume VATIN[2]; Bastien GANTY[2] ; Yves DETANDT[2]

[1] Acoustic laboratory, Montefiore Institute, University of Liège, Belgium

[2] Free Field Technologies, MSC Software Belgium, Belgium

ABSTRACT

Strong insulation in modern buildings and housing requires efficient ventilation systems. A popular solution is a decentralized system with one ventilation unit per room, but the noise emitted by such a unit then has a major impact on the comfort. In this research, it is intended to equip an existing ventilation unit with an active noise control (ANC) system to reduce its low-frequency noise emissions. The ANC system will be hosted in an additional duct deporting the air inlet aperture approximately one meter away from its original position. The one-channel feedforward ANC system has a reference microphone located between the fan and the anti-noise loudspeaker and an error microphone at the duct's end. The transfer functions have been computed by a 3D FEM solver, between the fan and several reference and error microphone locations. Several combinations of reference/error microphone positions were then tested regarding the possible active attenuation of a white noise emitted by the primary source. Optimal control by the ANC controller was assumed, the optimal filter being computed with the help of the corresponding transfer functions. Theoretical attenuations were obtained and optimal positions were finally defined for the two microphones of the ANC system. The first results are finally discussed in this paper and raise some questions regarding the influence of the noise spectrum on the attenuations obtained.

Keywords: 3D FEM, Active noise control, feedforward ANC

1. INTRODUCTION

Todays' new standards in buildings require eco-friendly ventilation systems delivering fresh air in quiescent places. The noise level emitted by these ventilation systems is therefore a key point in the selection of the system. An objective of the *Silenthalpic* research project is to reduce the noise emitted by a decentralized system, using passive as well as active techniques.

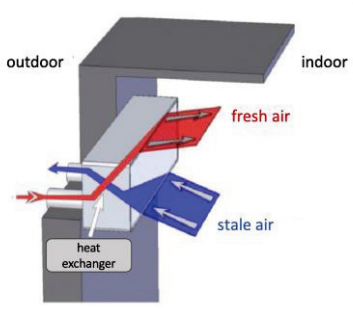

Figure 1 – Principle of a decentralized ventilation system

Decentralized systems are units composed of a casing containing one or two fans, a heat exchanger, filters and control electronics. The whole setup is installed at the top of a window or simply against a wall with two drilled holes. A schematic representation of the system is shown in Figure 1. In a

[1] s.lesoinne@uliege.be
[2] guillaume.vatin@fft.be

double-flux system, the two fans operate at the same time, enforcing the expected air flow rate of fresh and waste air. As the solution is decentralized, fans are in the actual living rooms and the noise generated must be limited.

The acoustic improvements of the design require a deep understanding of the noise sources characteristics and the acoustic transmission properties of the different components of the ventilation unit. In this respect, a numerical acoustic model of the ventilation unit was built which allows to compute the whole pressure field (spatial and frequency dependence) inside the unit. This model will be described in section 2. In particular, it will provide access to the acoustic transfer functions between single point sources located at the fan positions and any pre-defined microphone location.

Active noise control (ANC) solutions consist in the generation of secondary sound waves interfering negatively with the primary noise in order to reduce its amplitude in a given region of space (1). One of the most classical and efficient ANC method to reduce fan noise is the one-channel or multichannel feedforward control in a duct (1,2). This method is of course directly applicable in a centralized ventilation system, but not in a decentralized one in which the propagation paths followed by the emitted waves inside the unit are too complex. Also, the space available inside the unit for a feedforward ANC system is much too restricted.

Figure 2 – Front face of the ventilation unit (initial configuration)

Figure 2 shows a picture of the front face of the ventilation unit in its initial configuration. A preliminary acoustic diagnosis of this module has revealed that the most significant noise source was the stale air extraction aperture situated on the right, in front of the microphone in figure 2. It was therefore decided to install an additional component to the unit, consisting of a duct deporting the air inlet aperture to the left and including the ANC system. A one-channel feedforward controller will be implemented inside the duct, with a reference microphone close to the initial air aperture, a control loudspeaker as secondary source and an error microphone close to the new deported aperture.

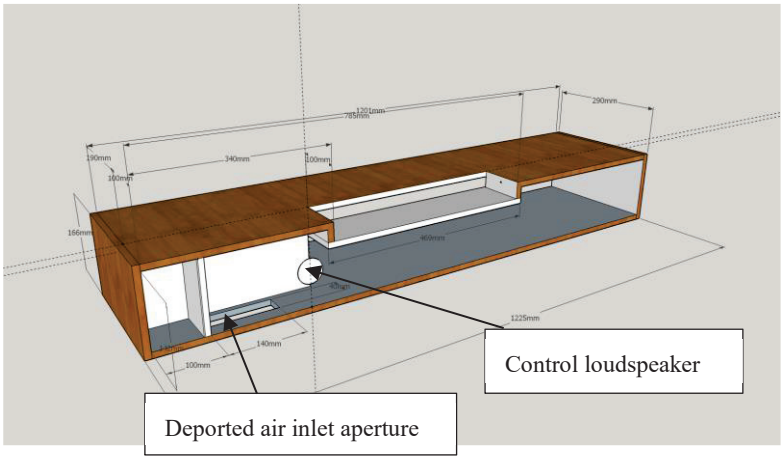

Figure 3 – Schematic internal view of the additional duct

Figure 3 is a schematic internal view of this additional duct in which the front face of the unit will

be embedded. The total length of the duct (1.1m) allows a sufficient propagation delay between the reference microphone and the control source, leaving enough time for the controller to compute the anti-noise signal. Also, the cross-section dimensions insure that mostly plane waves propagate inside the duct at frequencies smaller than 1.2 kHz, justifying the choice of a one-channel ANC system.

2. NUMERICAL ACOUSTIC MODELLING OF THE VENTILATION UNIT AND COMPUTATION OF THE TRANSFER FUNCTIONS

The location of the reference microphone, the control loudspeaker and the error microphone may have an important effect on the performance of the feedforward ANC system. Acoustic simulation can be used to evaluate the transfer functions between the primary and secondary sources on one hand, and many virtual microphone locations on the other hand. This allows to determine the positions of the reference and error microphones leading to the best efficiency of the ANC system. This section describes the numerical modelling of the ventilation unit used to compute such transfer functions.

Acoustic simulations are performed using Actran, a finite element-based modelling software developed by Free Field Technologies. Starting from a CAD (Computer Aided Design) geometry of the ventilation unit and the additional duct, the air volumes inside the module and the duct are meshed using linear tetrahedral elements. The Figure 4 below shows the cavities mesh (inner air volumes) created from a CAD geometry.

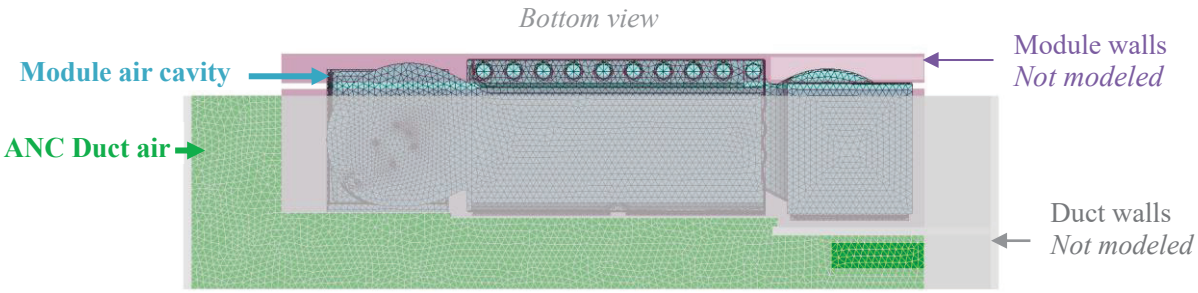

Figure 4 - Inner air volumes in numerical model

Additionally, a part of the air around the whole system is meshed on both sides of the system and non-reflective boundary conditions are defined to model free-field propagation. Acoustic waves then are free to propagate outside of the system through ventilation module's apertures towards exterior side and the duct's aperture towards interior side. The structural parts are not modelled, which means that inner air domains' boundaries are assumed to be purely reflective (equivalent to rigid walls). No damping is considered. Property of fluid domains is air at atmospheric pressure and ambient temperature (340m/s for speed of sound, 1.225kg/m³ for the density). The elements of the mesh are sufficiently small to ensure an accurate numerical computation of the acoustic transfer functions up to 1 kHz.

The primary source is modeled by a monopole source with unitary amplitude which generates 1 Pascal at 1 meter. Flow-induced noise is not taken into account in the model.The primary source can alternatively be located at one of the two fans' positions. The control loudspeaker excitation is modeled using a unitary acoustic velocity boundary condition. Three loudspeaker positions are assessed (see Figure 5). Such modelling of the excitations is appropriate for acoustic transfer function computation, knowing that plane waves propagate in the module and the ANC duct at the frequencies of interest.

A grid of virtual microphones is then defined in the ANC duct volume to compute the transfer functions between the sources and multiple locations of potential reference and error microphones.

Virtual microphones are also added near the duct aperture and in the far field (Figure 7). Microphones in the far field are used to evaluate the efficiency of the ANC system not only at the error microphone, but also at remote distance from the module.

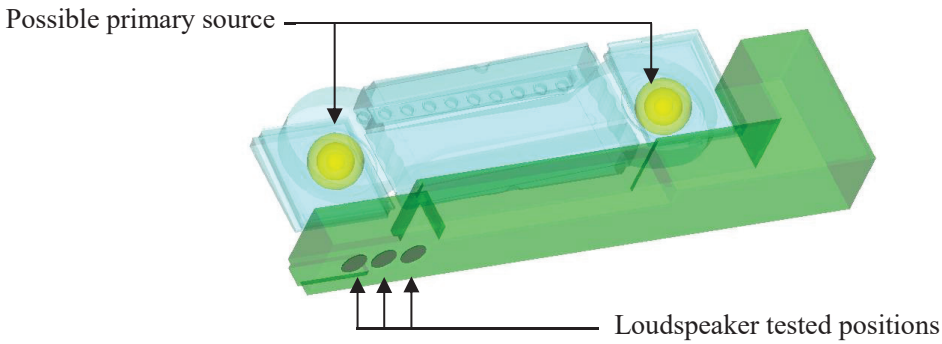

Figure 5 - Primary source position and secondary source positions

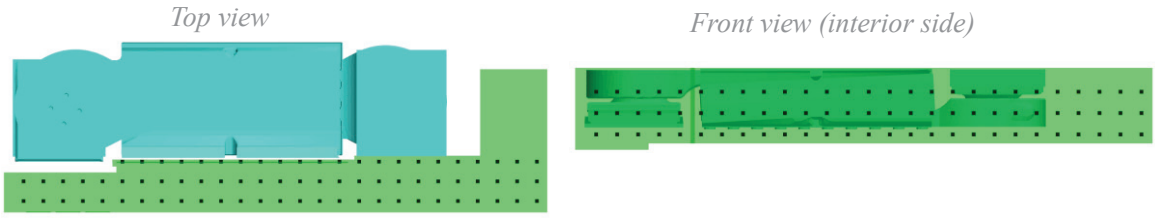

Figure 6 - Grid of virtual microphones in duct

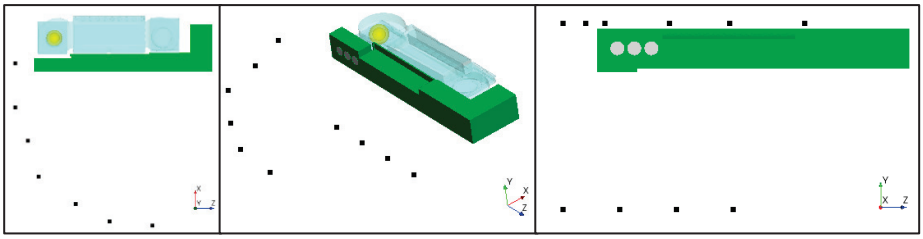

Figure 7 – Far-field microphones

The real and imaginary part of the pressure is computed up to 1kHz at each virtual microphone and for all load cases (primary sources and loudspeaker). As unitary values are set for the excitations, such pressure results correspond to the acoustic transfer functions between source and microphone and they can be used to calibrate the ANC module.

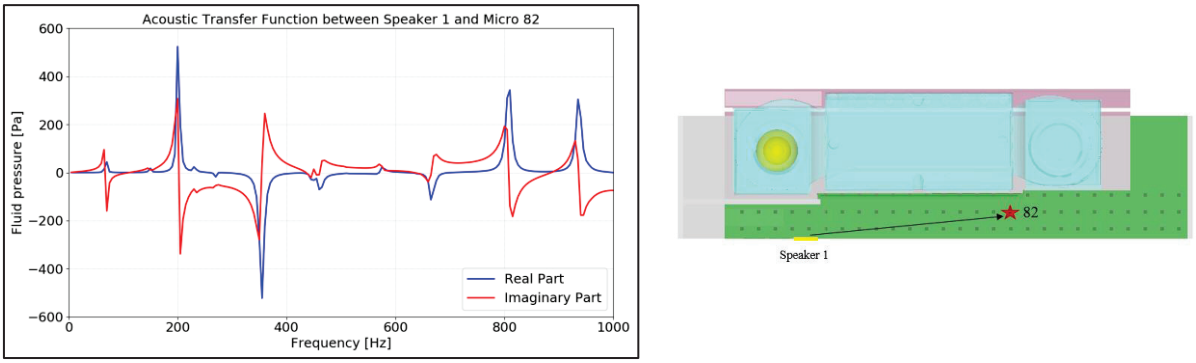

Figure 8 - Example of acoustic transfer function provided

3. SIMULATION OF OPTIMAL ACTIVE NOISE CONTROL

3.1 Method

It is intended in the *Silenthalpic* research project to implement and test a feedforward one-channel ANC system inside the additional duct shown in Figure 3. The performance of such system depends particularly on the positions of the two microphones (reference and error microphones) and the control loudspeaker (1). As mentioned in the previous section, these positions could be optimized by the application of a model of the pressure fields created by the fans and the control loudspeaker inside the duct. The optimized positions are those which minimize the absolute value of the total pressure at the error microphone.

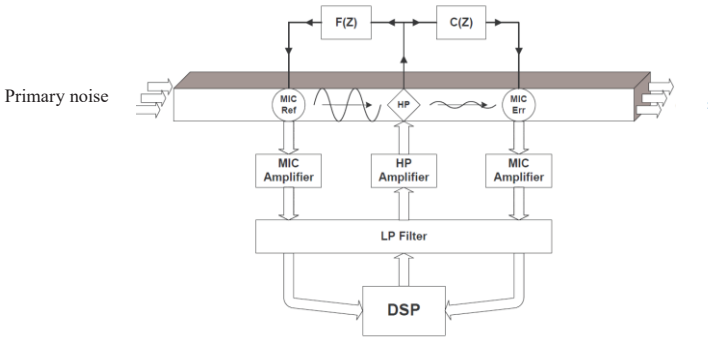

Figure 9 – Feedforward ANC system

The pressure field generated by the control loudspeaker depends on the anti-noise signal computed by the controller. A model of the controller is therefore also necessary: in this study, the model of optimal control described by Nelson and Elliot (1) is used. In this model, the transfer function of the optimal controller is:

$$H_{opt}(\omega) = -S_{rd}(\omega)/S_{rr}(\omega) \tag{1}$$

In which $S_{rd}(\omega)$ is the cross-spectral density of the primary noise $D(\omega)$ measured at the error microphone and the filtered-reference signal $R(\omega)$, while $S_{rr}(\omega)$ is the power spectral density of $R(\omega)$. The filtered-reference signal is the one measured at the reference microphone, filtered by the 'error path' $C(\omega)$ simulating the transfer function between the control loudspeaker and the error microphone (1): see Figure 9.

However, this model is in some way an 'ideal' case. In particular, the transfer function expressed by Eq.(1) could be non-causal. Nelson and Elliot (1) therefore suggest to design the optimal filter $H_{opt}(\omega)$ in the time domain, as a causal FIR filter. The number of coefficients of this filter is a parameter of the method. Once again, the optimal controller is the one which minimizes the power of the signal at the error microphone. To simplify the search of the optimal FIR filter, the feedforward controller is assumed to exactly compensate the feedback effect of the control loudspeaker at the reference microphone (feedback noted $F(z)$ in Figure 9). If the vector $\vec{h}$ represents the set of the FIR filter's coefficients (h_0, h_1, …h_{K-1}, size K) and the vector $\vec{\rho}$ (size K) is such that ρ_k is the expectation of the product $(r[n]d[n+k])$, then the optimal filter is defined in the time domain by (1):

$$\vec{h}_{opt} = R^{-1}\vec{\rho} \tag{2}$$

In this definition, $r[n]$ is the filtered-reference signal, $d[n]$ is the primary noise measured at the error microphone and R is a square matrix of size K^2 whose element R_{ki} is the expectation of the product $(r[n]r[n+|k-i|])$. These elements can be evaluated if the signal at the reference microphone $x[n]$ is a white noise. Indeed, according to the definition of $r[n]$ which is the convolution of $x[n]$ with the filter c_k (representing the 'error path' $C(z)$, size L):

$$E\{r[n]r[n+m]\} = E\left\{\sum_{k=0}^{L-1} c_k x[n-k] \sum_{u=0}^{L-1} c_u x[n+m-u]\right\} = \overline{X^2} \sum_{k=0}^{L-1} c_k\, c_{k+m} \tag{3}$$

In Eq.3, $\overline{X^2}$ represents the power of the white noise $x[n]$. By the same way, if we define the filter p_k

(size L) as the propagation path between the reference and the error microphones, then:

$$E\{r[n]d[n+m]\} = E\left\{\sum_{k=0}^{L-1} c_k x[n-k] \sum_{u=0}^{L-1} p_u x[n+m-u]\right\} = \overline{X^2} \sum_{k=0}^{L-1} c_k \, p_{k+m} \quad (4)$$

In the following, we can set $\overline{X^2} = 1$ without loss of generality. The impulse response of the filters c_k and p_k will be evaluated from the transfer functions obtained with the numerical model described in section 2. Finally, Eq.2 gives the optimal filter and the minimized error signal is:

$$e[n] = d[n] - \sum_{k=0}^{K-1} h_{opt,k} \, r[n-k] \quad (5)$$

3.2 Implementation

In the numerical model, the pressure field has been computed on a grid of possible microphone positions, distributed in the interior volume of the duct (see section 2). In each cross-section of the duct (every 4cm along the duct's axis), six or nine microphone positions are defined, leading to a total of 228 possible microphone positions. Some of these positions were preferentially considered as 'error' microphone positions and others as 'reference' microphone positions. The pressure field is known at each point of this grid for a monopolar source situated at a fan position inside the ventilation unit and for the control loudspeaker.

The 'error path' c_k or $C(\omega)$ is given by the pressure at the error microphone position, created by the control loudspeaker. The filter p_k or $P(\omega)$ is evaluated in the frequency domain by the ratio of the complex pressures generated by the monopolar source at the error and reference microphone positions. Indeed, the primary noise $D(\omega)$ is (in the frequency domain) the product of the signal's spectrum S_ω and the transfer function $TE(\omega)$ between the primary noise source and the error microphone. In the same way, the primary noise $X(\omega)$ at the reference microphone is $S_\omega.TR(\omega)$, where $TR(\omega)$ is the transfer function between the primary noise source and the reference microphone. Therefore, we have that:

$$D(\omega) = S_\omega \, TE(\omega) = X(\omega)\frac{TE(\omega)}{TR(\omega)} = X(\omega)P(\omega) \quad (6)$$

Two problems must be solved before exploiting these filters in the computation of the optimal filter through eq.(2-5). The first problem is a too low spectral resolution for some transfer functions. As the numerical model has computed the complex pressure every 5 Hz (until 1 kHz), the impulse response obtained by IFFT is not longer than 200ms. For some transfer functions, this length is not sufficient, leading to significant time aliasing effects created during the IFFT operation. This first problem was solved by an interpolation to obtain a pressure value every 1 Hz (until 1 kHz), leading to impulse responses as long as 1s. Figure 10 shows the example of an impulse response truncated at 200ms (with time aliasing) and the same impulse response after spectral interpolation.

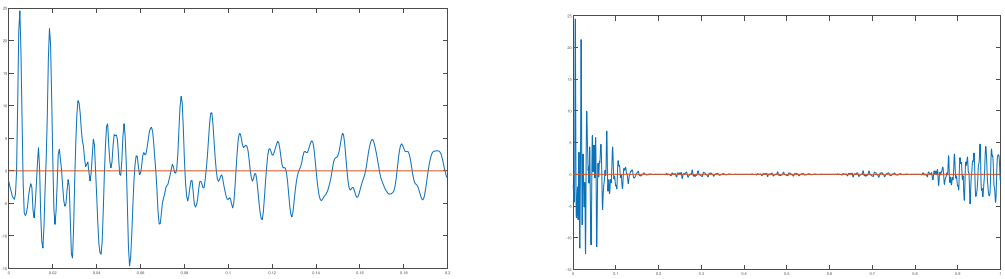

Figure 10 – Impulse response obtained with a spectral resolution of 5 Hz (left) and 1 Hz (right).

The second problem is that non-causal impulse responses are obtained by the inverse FFT of the complex pressures computed by the numerical model. This is also illustrated in Figure 10. To solve this problem, all the impulse responses (c_k or p_k) have been simply truncated at 500ms, removing the non-causal part. The effect of this simple solution has been analyzed in the frequency domain. Figure 11 shows for example the effect of removing the non-causal part of the response of Figure 10: the most significant impact is to reduce the amplitude of the pressure close to the resonance frequencies.

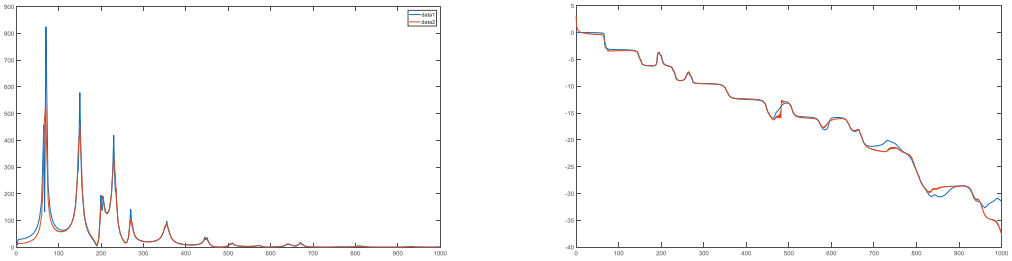

Figure 11 – Amplitude and phase spectra of the non-causal (in blue) and causal (in orange) versions of the same impulse response. The causal version is obtained after truncation at 500ms.

3.3 First results

The optimal control has been tested for the error microphone situated at positions number 199 to 228, in the vicinity of the new deported air inlet aperture. For each of these positions, the reference microphone was located at positions number 54 (the closest to the control loudspeaker) to 198 (the closest to the initial air aperture). A white noise spectrum is imposed to the pressure at the reference microphone, as in the procedure described in section 3.1. The attenuation obtained by the optimal controller at the error microphone is shown in Figure 12, as a function of both microphones' positions. The attenuations are computed on the whole frequency interval between 62.5 Hz and 1 kHz.

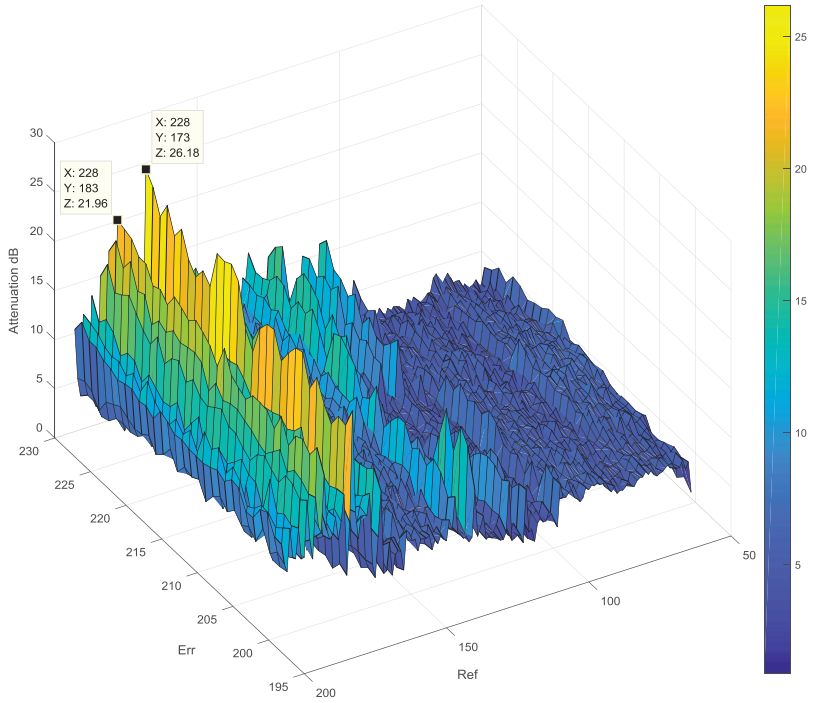

Figure 12 – Attenuation (dB) obtained at the error microphone by the optimal controller, for several pairs of error and reference microphone positions, referenced by their number (respectively 'Err' and 'Ref').

As shown in Figure 12, the attenuation is rather independent of the error microphone location (at least among the selected possible positions). On the contrary, an optimum position emerges for the reference microphone, identified by the number '173' which corresponds to a location close to the original air inlet aperture, in the upper part of the duct. An attenuation of more than 25 dB is predicted

at that position.

As the reference microphone is moved closer to the control loudspeaker, then the attenuation obtained at the error microphone decreases substantially.

We have also tested the influence of the primary noise spectrum on the controller's performance. If a white noise spectrum is now imposed at the source (fan), this means that the spectrum at the reference microphone is no longer a white noise. Indeed, one must include in the simulation the acoustic transfer function between the fan and the reference microphone position. As a result, the attenuation obtained at the error microphone drops to less than 10 dB at the optimum position (which is still number '173'). At other positions, the attenuations obtained in this case also decrease.

4. CONCLUSIONS

This paper describes the use of a 3D-FEM numerical model of a decentralized ventilation unit to optimize the positions of sensors and actuators of a feedforward ANC system. The unit is equipped with an additional duct covering its original front face and hosting the microphones and control loudspeaker of the ANC system.

The numerical model has been built with Actran to obtain the acoustic transfer functions between several pairs of source and microphone positions. These functions have been transformed by IFFT into impulse responses to simulate an optimal control strategy.

The first results have shown the existence of an optimal position for the reference microphone, but the attenuations were rather independent from the error microphone's position (restricted in a given zone around the air inlet aperture at the end of the duct). Also, the performance at the optimal position depends on the spectrum of the noise.

These first results of course raise some questions which must be further analyzed. In particular, the non-causal component in the transfer function delivered by the numerical model should be avoided. Also, the definition of the filter $P(\omega)$ as the ratio of the pressure spectra at two microphone positions is questionable, as this implies the application of a white noise spectrum at a location inside the duct (at the reference microphone position) to compute the optimal filter. This is perhaps not the most appropriate method: a white noise or a real measured spectrum, including the pure tones emitted by the fan, directly applied at the fan position would perhaps be more realistic.

ACKNOWLEDGEMENTS

The authors would like to acknowledge the Walloon Region for the financial support of the research presented here, as part of the Silenthalpic project (C7711).

REFERENCES

1. Nelson PA, Elliott SJ. Active Control of Sound. Academic Press, London and USA:San Diego; 1992.
2. Laugesen S. Active control of multi-modal propagation of tonal noise in ducts. Jnl Sound Vib. 1996;195(1):33-56.